Composites Part B 107 (2016) 1–8

Contents lists available at ScienceDirect

Composites Part B

journal homepage: www.elsevier.com/locate/compositesb

The hygrothermal aging process and mechanism of the novolac epoxy resin

Man Wang [a, b], Xiaowei Xu [b], Jin Ji [b], Yang Yang [b], Jianfeng Shen [b, **], Mingxin Ye [a, b, *]

[a] Department of Materials Science, Fudan University, 200433, Shanghai, China
[b] Institute of Special Materials and Technology, Fudan University, 200433, Shanghai, China

ARTICLE INFO

Article history:
Received 6 June 2016
Received in revised form
26 August 2016
Accepted 22 September 2016
Available online 22 September 2016

Keywords:
Novolac epoxy resin
Hygrothermal aging
Moisture absorption
Relative humidity

ABSTRACT

Novolac epoxy resins, with the high glass transition temperature (T_g) and excellent mechanical strength, are widely applied in the molding and sealing compounds for the production of electronic devices. However, weather exposure and environmental elements are inclined to affect their durability severely. This work focuses on the hygrothermal aging process and mechanism of the novolac epoxy resin. The effect of humidity and time in hygrothermal aging on structural and mechanical properties of the novolac epoxy resin was deeply studied. The moisture absorption increases linearly with the square root of aging time, and it follows the Fick's second law. There are two main categories of reactions in hygrothermal aging: the first one is the post curing process, which leads to a larger crosslinking density and a reduced interior stress; while the other is the plasticization and deterioration of epoxy resin attributed to moisture ingress. The combination of above factors leads to a decrease-increase-decrease variation in mechanical properties. This work is believed to benefit the wide and safe application of a certain novolac epoxy resin system in engineering application.

1. Introduction

Resin matrix composites boast high specific strength, favorable thermal and chemical stability, strong designability, and excellent fatigue resistance, and thus they are widely used in marine, offshore and civil infrastructure applications [1–5]. Amongst them, novolac epoxy resins, with the high glass transition temperature (T_g) and excellent mechanical strength, are widely employed in the molding and sealing compounds for the production of electronic devices [6–8].

In some certain application areas, environmental factors, such as heat, moisture, ultraviolet, and varied loads, or their combinations may degrade the material properties [2,9,10]. Weather exposure and environmental elements are inclined to affect the durability of materials severely [11]. And the environmental durability of materials is one of the limiting factors for their application [12]. While compared to the fiber in composites, the resin matrix is more susceptible to elevated temperature and humidity [13]. Much work has been done to investigate the effect of aging temperature on material properties [14–18]. In this work, we will pay more attention to the influence of varied humidity on the hygrothermal aging of a new type of epoxy.

The absorption of moisture penetrating from exposed surfaces induces both reversible and irreversible changes in material constituents and properties. Reversible changes are physical variations in nature, involving both property and dimensional changes [19,20]. Some aging effects such as softening and plasticization, can be recoverable at the initial stage of hygrothermal aging when the absorbed water is eliminated and no chemical reaction occurs [21,22]. While prolonged environmental exposure leads to permanent irreversible property alterations. The different possible competitive mechanisms which establish the durability during hygrothermal are: (a) additional cross-linking due to residual curing, (b) secondary cross-linking between the polymer chains and the water molecules, (c) swelling, (d) micro-cracking, (e) leaching of low molecular weight segments (decomposition), (f) plasticization, (g) polymer relaxation, etc. [14,19,23–26].

In hygrothermal process, water uptake process changes with temperature and humidity. Both of them influenced the diffusion coefficient and equilibrium moisture absorption content [16,17,27].

* Corresponding author. Department of Materials Science, Fudan University, 200433, Shanghai, China; Institute of Special Materials and Technology, Fudan University, Shanghai, China.
** Corresponding author. Institute of Special Materials and Technology, Fudan University, Shanghai, China.
E-mail addresses: jfshen@fudan.edu.cn (J. Shen), mxye@fudan.edu.cn (M. Ye).

http://dx.doi.org/10.1016/j.compositesb.2016.09.067
1359-8368/

T_g can be regarded as the most useful parameter revealing material degradation [28]. A decrease in T_g is generally attributed to plasticization and deterioration, while an increase in T_g is derived from a post-curing phenomenon during hygrothermal process. Besides, Fourier transform infrared spectroscope (FT-IR), thermal gravimetric analysis (TGA), and dynamic thermomechanical analysis (DMA) can be adopted to analyze the constituent and structure changes in resin molecules during the whole process of aging [14,29–31]. Mechanical tests can be conducted to study the variation of strength and modulus [9,10,27,32–35]. In addition, scanning electronic microscopy (SEM) can help to study the micromorphology.

In this present study, a new type of cured novolac epoxy resin underwent a 28-day aging process at a constant temperature of 60 °C. To investigate the influence of humidity of hygrothermal aging, we carried out three sets of experiments, i.e., immersing a set of samples into deionized water (Case I), and placing two sets in the constant temperature humidity chamber with the relative humidity (RH) of 98% (Case II) and 65% (Case III), respectively. The duration of 0, 2 h, 6 h, 1 day, 3 days, 1 week, 2 weeks, and 4 weeks for each case were selected to study the impact of aging time. This work is expected to be helpful in understanding the effects of hygrothermal aging on the long term durability of epoxy resin in harsh service environment. It is believed to benefit the wide and safe application of a certain epoxy system.

2. Experimental procedure

2.1. Sample preparation

The novel material was a cured system of resin and rubber. Regarding the reactants, epoxy resin 618 (also called epoxy E51) and phenolic epoxy resin F-44 were purchased from Shanghai resin factory Co., Ltd., epoxy resin AFG-90, Andebao from Shanghai Huayi Resins Co., Ltd., and carboxyl-terminated butadieneacrylonitrile (CTBN) from Shenzhen Jiadida Chemical Co., Ltd. Above four materials were cured with the assistance of the curing agent, 4, 4′-diaminodiphenyl sulfone (DDS) and the accelerator, triphenyl phosphine (PPh_3), both of which were bought from Sinopharm Chemical Reagent Co., Ltd. These chemical agents were used without further purification.

The epoxy resin 618, phenolic epoxy F-44, epoxy resin AFG-90, and CTBN with the weight ratio of 9:6:4:1 as well as some certain PPh_3 were added into a 1000 mL flask and mechanically stirred at 125 °C for 48 h 100 g above resin/rubber mixture and 32.27 g DDS were blended and mechanically stirred at 170 °C for 15 min. Afterwards, they were poured into a mold with a cavity of 160 mm × 150 mm × 5 mm in a 170 °C oven for 2 h. The samples were further sectioned with a universal cutting machine (WZY-240, China) into the dimension to the requirements of following tests.

2.2. Hygrothermal aging process

The samples of Case I were immersed in deionized water at 60 °C. While the hygrothermal aging for Case II and Case II were performed in the constant temperature and humidity test machine (CZ-A-408G, Shanghai, China) at 60 °C with the relative humidity of 98% and 65% respectively. Eight kind of aging time of 0, 2 h, 6 h, 1 day, 3 days, 1 week, 2 weeks, and 4 weeks for Case I (immersed in water), Case II (RH = 98%), and Case III (RH = 65%) were carefully characterized and analyzed in this study.

2.3. Gravimetric measurement

Twelve specimens (35 mm × 35 mm × 3 mm) were applied for each case. Before hygrothermal aging, the weight of each sample W_0 was measured and recorded. At the time point of 0, 2 h, 6 h, 1 day, 3 days, 1 week, 2 weeks, and 4 weeks, in the aging process, samples were taken out of the constant temperature humidity chamber, wiped dry with tissue paper and weighed by an electronic scale with a precision of 0.01 mg. And then they were quickly put back in the chamber again for further hygrothermal aging. The average weight and the standard deviation of twelve specimens were recorded and calculated.

The moisture absorption content M_t is defined in Equation (1):

$$M_t(\%) = \frac{W_t - W_0}{W_0} \times 100 \quad (1)$$

where W_t and W_0 are the sample weights at time t and initial state, respectively.

2.4. FT-IR

The samples aged for 28 days in Case I, Case II, and Case III together with the unaged resin were analyzed on an FT-IR spectroscope (Nicolet IS10, the USA) over a wave number range of 4000 to 400 cm^{-1} with a resolution of 4 cm^{-1}. The FT-IR samples were pressed together with KBr powder.

2.5. TGA

The specimens aged in three cases after 28 days and unaged resin were conducted thermo-gravimetric analysis on a Netzsch TG 209F1 (Germany) with the nitrogen purging. The samples were heated from room temperature to 900 °C, at a heating rate of 10 °C/min.

2.6. Tensile property test

In order to study the influence of the humidity and the duration time of hygrothermal aging on the tensile properties, a tensile test was performed on the Mechanical testing machine (MTS, CMT5105, the USA) with a crosshead speed of 1 mm/min. At least five specimens for each duration time and each case were conducted and recorded. Note that the sample dimension was 250 mm × 15 mm × 3 mm.

2.7. Flexural property test

The three-point bending test was carried out by the MTS CMT5105 (the USA) with a crosshead speed of 1 mm/min and the support span of 48 mm. At least five specimens for each duration time and each case were conducted and recorded. Note that the sample dimension was 60 mm × 10 mm × 3 mm.

2.8. DMA

DMA of the epoxy samples for each time and each case was performed in three-point bending mode on NETZSCH DMA 242 (Germany) at a frequency of 1.0 Hz, with a heating rate of 10 °C/min from 30 °C to 210 °C. At least three specimens for each duration time and each case were conducted and recorded. Note that the sample dimension was 50 mm × 10 mm × 3 mm.

2.9. SEM

The tensile fracture surface of specimens aged in three cases after 28 days and the unaged resin were observed on a scanning electron microscope (Tescan MAIA3 XMH, Czech). Data were

collected at the accelerating voltage of 5.0 kV and working distance of about 5 mm. Prior to the characterization of SEM, the samples were sputter-coated with a thin layer of gold in vacuum to improve the electrical conductivity.

3. Results and discussion

3.1. Moisture absorption analysis

The plots of the moisture absorption content versus the square root of hygrothermal aging time of three cases are presented in Fig. 1. The moisture absorption increases linearly with the square root of aging time, indicating that it follows the Fick's second law [36,37]. Generally, moisture sorption behaviors in polymers conform to Fickian diffusion as depicted in Equation (2).

$$\frac{M_t}{M_m} = 1 - \sum_{n=0}^{\infty} \frac{8}{(2n+1)^2\pi^2} \exp\left[-\frac{D(2n+1)^2\pi^2 t}{4h^2}\right] \quad (2)$$

where M_t is the moisture absorption content at time t, M_m is the equilibrium value of the diffusing water, D is the diffusion coefficient, and h is the sample thickness.

For $Dt/h^2>0.05$, the above equation reduces to Equation (3):

$$\frac{M_t}{M_m} = 1 - \frac{8}{\pi^2} \exp\left(-\frac{Dt}{h^2}\pi^2\right) \quad (3)$$

For $Dt/h^2<0.05$, the above equation reduces to Equation (4):

$$\frac{M_t}{M_m} = \frac{4}{h}\sqrt{\frac{Dt}{\pi}} \quad (4)$$

From Equation (4), the diffusion coefficient D, which is a significant parameter in Fick's law, can be calculated from the slope of the water absorption curves versus square root of time [12,38]. The values of D and M_m in the present study are summarized in Table 1. As shown, both the equilibrium moisture absorption content and the diffusion rate follow the same pattern that Case I > Case II > Case III, in other words, higher relative humidity contributes to severer water absorption. We can conclude that raising the humidity of the environment accelerates the penetration of water molecules into the polymers. This indicates that the water diffusion into the novolac epoxy resins is controlled by the activity of the water, which is further influenced by the relative humidity.

Table 1
The equilibrium moisture absorption content M_m and the coefficient of diffusion (D) of the resin in Case I, Case II and Case III.

Parameter	Case I	Case II	Case III
M_m (%)	3.13	2.88	1.12
$D \times 10^7$ (mm^2 s^{-1})	7.60	7.55	7.21

3.2. FT-IR analysis

It is widely known that the aging may take place at the molecular level with distinctive changes in the chemical structures [39]. To investigate the chemical molecular variations, we conducted the FT-IR spectra of specimens aged in three cases after 28 days and the unaged sample (Fig. 2). The assignments of the characteristic absorption bands are shown in Table 2.

As the order of unaged, Case III, Case II, and Case I after the 28-day hygrothermal process, the absorption band of O–H group between 3300 cm^{-1} and 3000 cm^{-1} enhances and moves toward higher wave numbers. It indicates more hydrogen bands association and more water absorption, which is consistent with the moisture absorption analysis [40].

In contrast, the absorption band intensity of N–H group between 3600 cm^{-1} and 3300 cm^{-1} decreases in the above order. The reason might be the post-curing process, during which the residual secondary amino groups further react with the curing agent. Besides, higher humidity contributes more to the completion of post-curing. The possible reaction is summarized in Scheme 1 [41,42].

Meanwhile, the intensity of the band near 2930 cm^{-1} weakens, indicating the oxidation of C–H in methylidyne groups [43]. The absorption reduction of the band near 1040 cm^{-1}, corresponding to the symmetrical stretching vibration of C-O-φ (φ represents benzene ring), indicates the destruction of C-O-φ during hygrothermal aging [44]. While the band near 1240 cm^{-1} becomes broadened and moves toward lower wave numbers, verifying the formation of φ-O-φ band [45,46]. The possible reaction of consumption of $-CH_2$ and production of φ-O-φ is shown in Scheme 2 [45].

3.3. TGA analysis

The effect of hygrothermal aging can also be perceived in the TGA test. Fig. 3a depicts the weight variation at the temperature range of 30 °C to 900 °C. As seen, the higher humidity it is, the

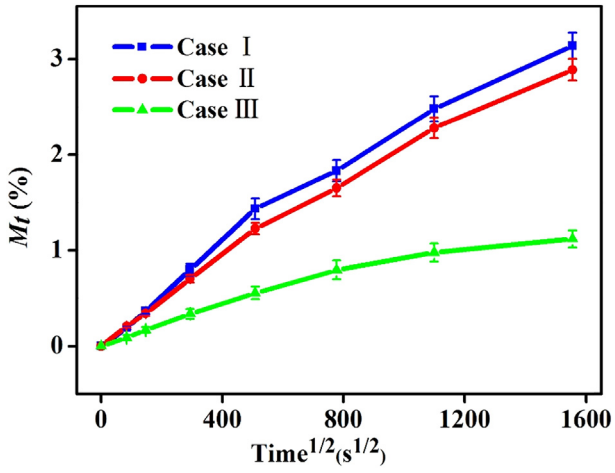

Fig. 1. The plots of the moisture absorption content versus the square root of hygrothermal time in Case I, Case II and Case III. Error bars represent the standard deviation due to twelve specimens for each aging time and each case.

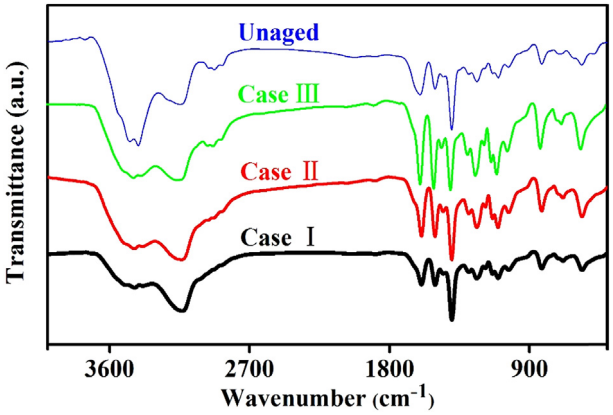

Fig. 2. The FT-IR Spectra of specimens aged for 28 days in three cases and the unaged sample.

Table 2
Assignments of the characteristic absorption bands in the FT-IR spectra.

Absorption bands (cm^{-1})	Assignment
3700–3300	Stretching vibration of N–H
3300–3000	Stretching vibration of O–H
2930	Stretching vibration of –C–H in methylidyne
1240	Asymmetrical stretching vibration of C-O-φ
1040	Symmetrical stretching vibration of C-O-φ

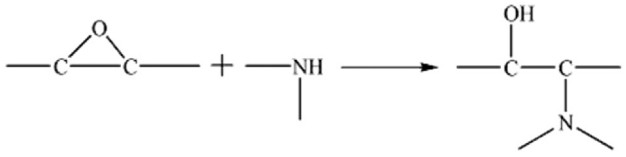

Scheme 1. Possible post-curing reaction.

system loses weight earlier and severer. Considering TGA plots before 150 °C overlap together, we magnified this portion and obtained Fig. 3b. At the temperature range of 30 °C to 150 °C, the sample weights decline smoothly when the resins went on the volatiles and moisture losses [31]. At 150 °C, the weight loss of Case I, Case II, and Case III are about 3.5%, 3.2%, and 1.5% respectively. For the moisture loss, the maximum water absorption ratio is 3.1%, 2.9%, and 1.1% in Fig. 1. The weight changes in Figs. 1 and 3 are in the same trend and with similar discrepancy. The difference of about 0.4% corresponds to the volatiles loss in resins [31]. The following phase exhibits the opposite tendency that the weight loss is delayed with the increase of relative humidity, which may be derived from the crosslinking and decomposition of the structure of resin molecules [47].

3.4. Tensile property analysis

The variation of the tensile strength versus the square root of time throughout the whole aging program is given in Fig. 4 and their absolute values are listed in Table 3. As shown, the general tendency is a short decrease, an increase and a second decrease till the end. From the time point of 6 h to the end of aging for each case, the retention of the tensile strength follows the same sequence that Case I < Case II < Case III. After the hygrothermal aging for 28 days, the tensile strength retention is 64.06%, 78.04% and 81.29%, respectively. Note that the tensile strength of unaged sample is 58.29 ± 1.66 MPa.

The degradation of the tensile strength can be attributed the plasticization and deterioration of the resin with the penetration of water molecules into the resin structure [32]. The plasticization of novolac epoxy resin starts at the beginning of the hygrothermal aging process, and it goes in the same trends as the water uptake content. Though the deterioration takes place a little later, it brings about extremely severe influence in the latter phase until the end. On the other hand, water ingress into the resin causes the relaxation of residual stress and the acceleration of post-curing, both of which may be responsible for the significant increase of the mechanical properties [48].

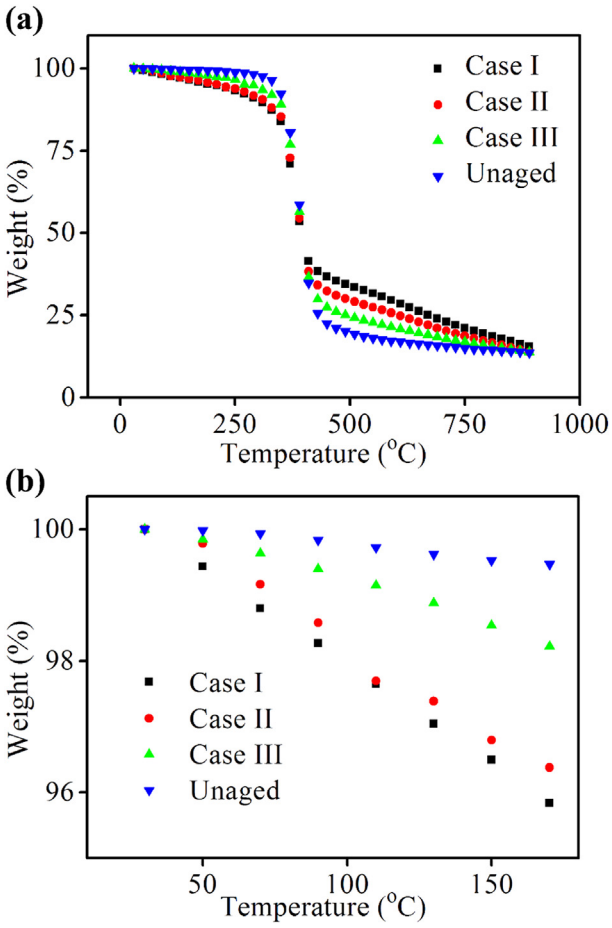

Fig. 3. TGA curves for unaged samples and those aged for 28 days in Case I, Case II and Case III of (a) the full temperature ranges and (b) at the temperature range of 30 °C to 150 °C.

With varied extent of above two categories of influencing factors, the system shows a diverse trend at different time. For Case I and Case II, there is a short and slight decrease in the first two hours, in which the water molecules act as the plasticization in the novolac epoxy resin and lead to a decreased strength; then the resin undergoes a sudden increase in tensile strength in the next four hours and the reason might be the severe post curing effect; after that, there exists a consecutive decrease in the following hygrothermal process, in which the resin is dramatically degraded by the water ingress and the deterioration overshadows the post curing effect [32,48]. As for Case III, there exhibit only an increase and a long decrease, without the first decrease phase in Case I and Case II. The reason may be that in the first several hours in case III, the water absorption is much less than the other two cases (Fig. 1), and the plasticization effect can't compare with the curing one [14].

3.5. Flexure property analysis

This part focuses on the variation of the flexure properties. The

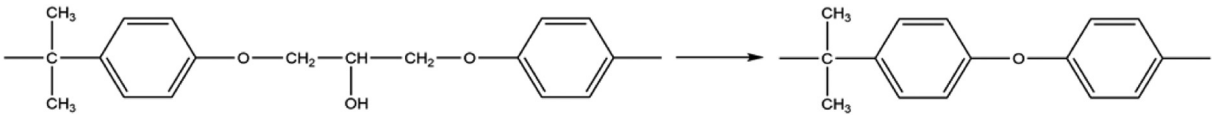

Scheme 2. Possible reaction producing φ-O-φ.

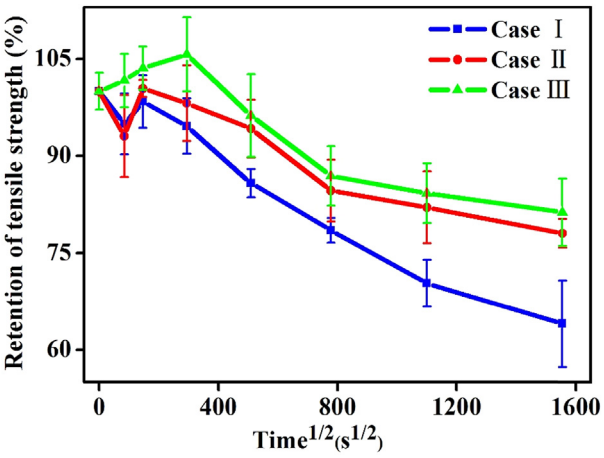

Fig. 4. The variation of the tensile strength retention as a function of the square root of the hygrothermal time throughout the whole aging program for Case I, Case II and Case III.

flexure strength and flexure modulus of three sets of samples versus the square root of time are given in Fig. 5a and b and their absolute values are listed in Table 3. The tendency is a general decrease with some slight increase in the initial several hours. After a hygrothermal time for 28 days, the flexure strength retention for each case is 75.27%, 77.30% and 82.79%; while the flexure modulus retention is 88.46%, 93.85% and 96.14%. Note that the flexure strength and flexure modulus of unaged sample are 141.19 ± 4.07 MPa and 2489.53 ± 46.43 MPa, respectively.

Just like tensile strength in hygrothermal process, there are two main opposite effects on the evolution of flexure properties simultaneously. The positive one is the post curing process, which leads to a larger crosslinking density and a reduced interior stress; while the negative factor is the deterioration and plasticization of epoxy resin attributed to moisture ingress [32,48].

For flexure strength in Case I, there is a continuous downtrend with a gradually reduced slope; while in case II and Case III, we can see a short decrease, followed by an increase and a second lasting

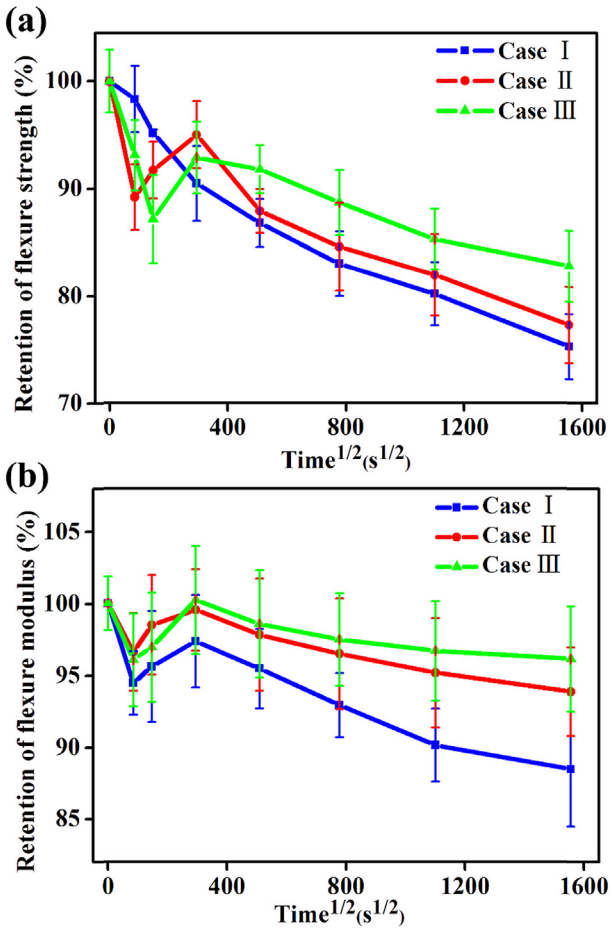

Fig. 5. The variation of the flexure strength (a) and flexure modulus (b) retention as a function of the square root of the hygrothermal time in Case I, Case II and Case III.

decrease till the end. In the hygrothermal stage of 2 h–24 h for case II and Case III, the post curing factor exerts more impact than the

Table 3
The tensile strength, flexure strength, flexure modulus and T_g of samples through the whole aging process for three cases.

Aging condition	The square root of aging time (s$^{1/2}$)	Tensile strength (MPa)	Flexure strength (MPa)	Flexure modulus (MPa)	T_g (°C)
Case I	0	58.3 ± 1.7	141.2 ± 4.1	2489 ± 46	168.8 ± 2.1
	85	55.3 ± 2.8	138.9 ± 4.4	2351 ± 55	167.4 ± 1.9
	147	57.4 ± 2.4	134.4 ± 0.5	2380 ± 96	172.3 ± 1.4
	294	55.1 ± 2.5	127.7 ± 5.0	2424 ± 80	169.3 ± 1.2
	509	50.0 ± 1.3	122.6 ± 3.2	2376 ± 69	165.8 ± 0.8
	778	45.8 ± 1.1	117.2 ± 4.3	2313 ± 55	152.3 ± 1.5
	1100	41.0 ± 2.1	113.2 ± 4.2	2244 ± 63	145.9 ± 1.9
	1555	37.3 ± 3.9	106.3 ± 4.3	2202 ± 100	143.9 ± 2.4
Case II	0	58.3 ± 1.7	141.2 ± 4.1	2490 ± 46	168.8 ± 2.1
	85	54.2 ± 3.7	125.9 ± 4.3	2405 ± 67	166.1 ± 1.8
	147	58.5 ± 0.8	129.5 ± 3.7	2452 ± 86	167.2 ± 2.3
	294	57.2 ± 3.4	134.2 ± 4.4	2478 ± 70	170.7 ± 1.8
	509	54.9 ± 2.6	124.1 ± 2.9	2435 ± 97	167.3 ± 1.3
	778	49.3 ± 2.8	119.4 ± 5.8	2402 ± 96	162.7 ± 2.4
	1100	47.8 ± 3.2	115.7 ± 5.4	2369 ± 95	158.7 ± 2.0
	1555	45.5 ± 1.3	109.1 ± 5.0	2336 ± 77	154.4 ± 1.4
Case III	0	58.3 ± 1.7	141.2 ± 4.1	2490 ± 46	168.8 ± 2.1
	85	59.3 ± 2.4	131.5 ± 4.6	2392 ± 80	164.2 ± 1.5
	147	60.4 ± 2.0	123.0 ± 5.8	2413 ± 94	165.3 ± 1.2
	294	61.6 ± 3.3	131.1 ± 4.7	2495 ± 94	169.3 ± 2.6
	509	56.1 ± 3.7	129.6 ± 3.2	2454 ± 93	168.2 ± 2.1
	778	50.7 ± 2.7	125.2 ± 4.3	2427 ± 80	164.8 ± 0.8
	1100	49.1 ± 2.7	120.4 ± 4.0	2407 ± 86	161.5 ± 1.3
	1555	47.4 ± 3.0	116.9 ± 4.7	2393 ± 91	160.0 ± 2.2

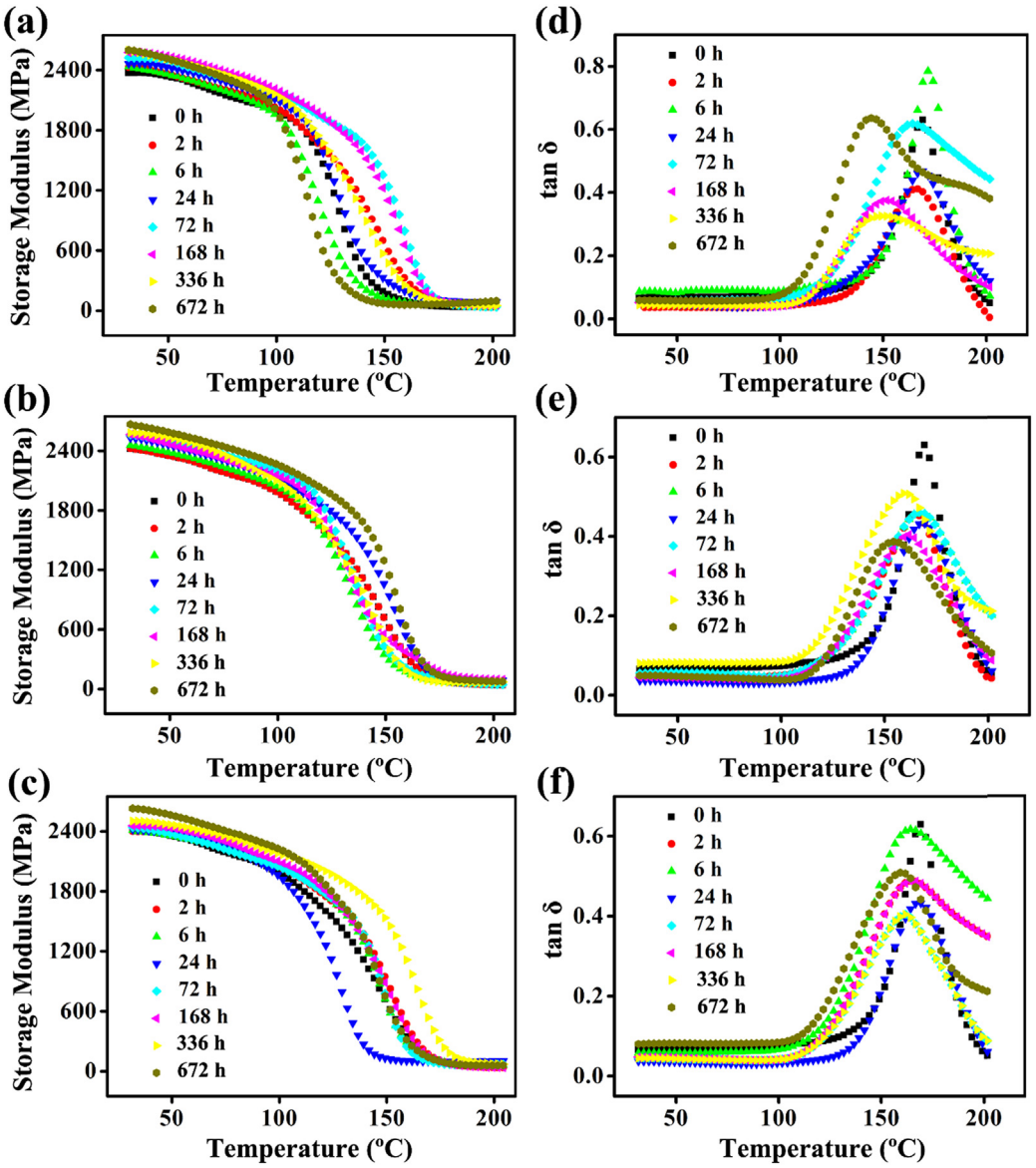

Fig. 6. The curves of the storage modulus E′ *vs.* temperature *t* for Case I (a), Case II (b) and Case III (c) and the curves of tan *δ* *vs.* temperature *t* for Case I (d), Case II (e) and Case III (f) at the time point of 0, 2, 6, 24, 72, 168, 336 and 672 h.

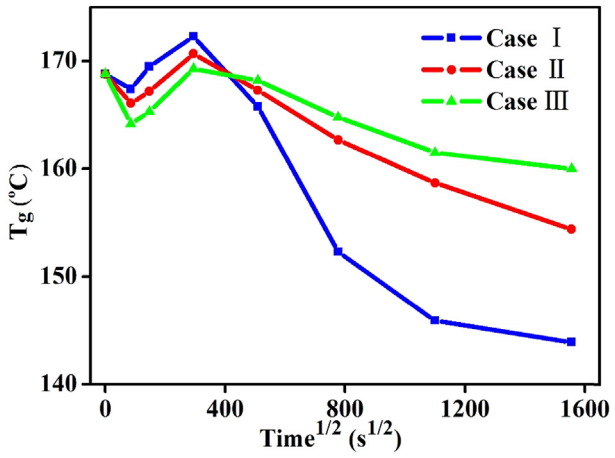

Fig. 7. The variation of T_g as a function of the square root of the hygrothermal time in Case I, Case II and Case III.

resin deterioration one with a small rise of flexure tensile. At other time in all cases, the resin plasticization and deterioration are the dominant factor, resulting in a continuous and prominent decrease in the hygrothermal course.

For flexure modulus in three cases, the general situation is a short decrease, a sequenced increase and a lasting decrease till the end. At the first two hours, the resin deterioration and plasticization play the leading role; and then, the post curing weights more; after 24 h, the resin deterioration influences the system more. With the combination of a series of factors, the resin system exhibits above tendency in flexure strength and flexure modulus.

3.6. DMA analysis

Fig. 6 shows DMA curves of three cases aged for 0, 2, 6, 24, 72, 168, 336 and 672 h. Fig. 6a, c and e depict the relations of storage modulus (E′) and temperature of Case I, Case II and Case III, exhibiting a characteristic step in the glass transition region. While

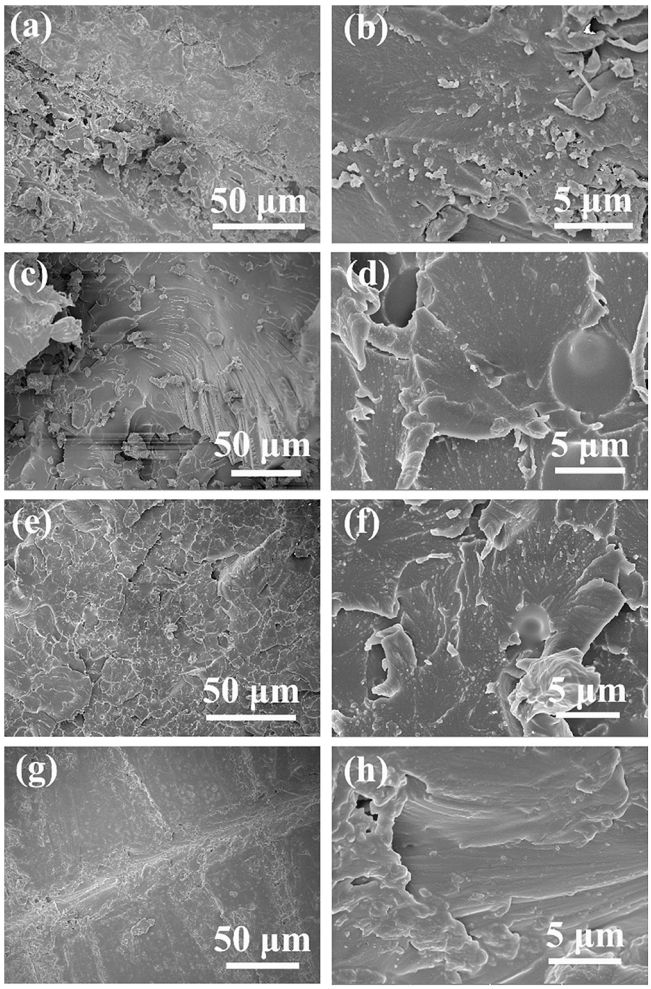

Fig. 8. SEM images of specimens aged for 28 days of Case I (a) and (b), Case II (c) and (d), Case III (e) and (f), and the unaged sample (g) and (h).

Fig. 6b, d and f present corresponding loss factor (tan δ) curves with a single peak in that region of Case I, Case II and Case III. The shapes of the DMA curves at the transition region reflect the resin change from a glassy state to an elastomeric state. Fig. 7 presents T_g variation obtained from DMA test throughout the whole aging program. The final column in Table 3 lists the T_g values of the aged materials. It undergoes a decrease-increase-decrease change in T_g.

The moisture content of a material can influence its thermo-mechanical properties and the variation of T_g is associated with changes in the chemical structure of the resin [49]. In the early stage of aging, the presence of moisture depressed T_g by acting as a plasticizer in the resin. Afterwards, the post-curing and leaching contributes to the increase of T_g. Here, the post-curing of resin lead to denser cross-linking and higher T_g; meanwhile, the second reason for this inversion of increased T_g is that small fragments acting as matrix plasticizers are leached out and cause the main chain to become less mobile [14]. Beyond a certain point, polymer undergoes a micro-cracking and degradation, resulting in a depressed T_g. As mentioned in Introduction, there are different possible competitive mechanisms which dominate in the establishing of the mechanical and visco-elastic behavior during hygrothermal aging. These fundamental mechanisms interplay with each other to generate the non-linear aging behavior [14,50,51].

3.7. SEM analysis

Fig. 8 shows the SEM images of the tensile fracture surface morphology. The left column contains the SEM graphs with a larger scope of the specimens aged for 28 days of Case I, Case II, Case III, and the unaged sample; while the right one corresponds to their smaller scope images with more detailed information. As shown, the surfaces of unaged specimens are relatively smooth without obvious particles or cracks (Fig. 8g–h). Meanwhile for three aged cases, there are a host of micro-cracks and particles in the surfaces (Fig. 8a–f), derived from the degradation of the polymers. Specifically speaking, the higher humidity it is, the more tiny nodules and crack propagation, indicating severer decomposition and deterioration of the resins [18,52–54].

4. Conclusions

This present work has studied the effect of humidity and time in hygrothermal aging on structural and mechanical properties of the novolac epoxy resin. It is found that moisture absorption behavior follows the Fick's second law. The characterization and analysis of FT-IR, TGA and DMA have informed us that during the hygrothermal aging process the novolac epoxy resin system has underwent two main categories of variations: 1) the first one is the post curing process, resulting in a larger crosslinking density and a reduced interior stress; 2) the other is the plasticization and deterioration of resin attributed to water ingress. The combination of above factors leads to a decrease-increase-decrease variation in mechanical properties, as seen in the results of tensile and flexure testing. While SEM graphs reveal the micro-crack and deterioration of resin in the aging course.

This work is expected to be helpful in understanding the effects of hygrothermal aging on the durability of epoxy resin in harsh service environment. It is believed to benefit the wide and safe application of a certain novolac epoxy resin system in engineering application.

References

[1] Lu Z, Xian G, Li H. Effects of thermal aging on the water uptake behavior of pultruded BFRP plates. Polym Degrad Stab 2014;110:216–24.
[2] Dogan A, Atas C. Variation of the mechanical properties of E-glass/epoxy composites subjected to hygrothermal aging. J Compos Mater 2015;50(5):637–46.
[3] Deng J, Shi W. Synthesis and effect of hyperbranched (3-hydroxyphenyl) phosphate as a curing agent on the thermal and combustion behaviours of novolac epoxy resin. Eur Polym J 2004;40(6):1137–43.
[4] Shin P-S, Wang Z-J, Kwon D-J, Choi J-Y, Sung I, Jin D-S, et al. Optimum mixing ratio of epoxy for glass fiber reinforced composites with high thermal stability. Compos Part B Eng 2015;79:132–7.
[5] Karbhari VM, Xian G. Hygrothermal effects on high VF pultruded unidirectional carbon/epoxy composites: moisture uptake. Compos Part B Eng 2009;40(1):41–9.
[6] Atta AM, Shaker NO, Nasser NE. Synthesis of bisphenol a novolac epoxy resins for coating applications. J Appl Polym Sci 2008;107(1):347–54.
[7] Free-volume characteristics and water absorption of novolac epoxy resins investigated by positron annihilation. Polymer. 37(14):6.
[8] Suzuki T, Oki Y, Numajiri M, Miura T, Kondo K, Shiomi Y, et al. Novolac epoxy resins and positron annihilation. J Appl Polym Sci 1993;49(11):1921–9.
[9] Guermazi N, Elleuch K, Ayedi HF, Kapsa P. Aging effect on thermal, mechanical and tribological behaviour of polymeric coatings used for pipeline application. J Mater Process Technol 2008;203(1):404–10.
[10] Aldajah S, Alawsi G, Rahmaan SA. Impact of sea and tap water exposure on the durability of GFRP laminates. Mater Des 2009;30(5):1835–40.
[11] Boubakri A, Elleuch K, Guermazi N, Ayedi HF. Investigations on hygrothermal aging of thermoplastic polyurethane material. Mater Des 2009;30(10):3958–65.
[12] Gkikas G, Douka DD, Barkoula NM, Paipetis AS. Nano-enhanced composite materials under thermal shock and environmental degradation: a durability study. Compos Part B Eng 2015;70:206–14.
[13] Yang Y, Xian G, Li H, Sui L. Thermal aging of an anhydride-cured epoxy resin. Polym Degrad Stab 2015;118:111–9.
[14] Cabral-Fonseca S, Correia JR, Rodrigues MP, Branco FA. Artificial accelerated

ageing of GFRP pultruded profiles made of polyester and vinylester resins: characterisation of physical–chemical and mechanical damage. Strain 2012;48(2):162–73.
[15] Aït Oumeziane Y, Moissette S, Bart M, Lanos C. Influence of temperature on sorption process in hemp concrete. Constr Build Mater 2016;106:600–7.
[16] Guermazi N, Ben Tarjem A, Ksouri I, Ayedi HF. On the durability of FRP composites for aircraft structures in hygrothermal conditioning. Compos Part B Eng 2016;85:294–304.
[17] Park Y-B, Kweon J-H, Choi J-H. Failure characteristics of carbon/BMI-Nomex sandwich joints in various hygrothermal conditions. Compos Part B Eng 2014;60:213–21.
[18] Firdosh S, Narasimha Murthy HN, Pal R, Angadi G, Raghavendra N, Krishna M. Durability of GFRP nanocomposites subjected to hygrothermal ageing. Compos Part B Eng 2015;69:443–51.
[19] Starkova O, Buschhorn ST, Mannov E, Schulte K, Aniskevich A. Water transport in epoxy/MWCNT composites. Eur Polym J 2013;49(8):2138–48.
[20] Lassila LVJ, Nohrström T, Vallittu PK. The influence of short-term water storage on the flexural properties of unidirectional glass fiber-reinforced composites. Biomaterials 2002;23(10):2221–9.
[21] Zhou J, Lucas JP. Hygrothermal effects of epoxy resin. Part II: variations of glass transition temperature. Polymer 1999;40(20):5513–22.
[22] Pochiraju KV, Tandon G, Schoeppner GA. Long-term durability of polymeric matrix composites. Springer Science & Business Media; 2011.
[23] Sousa JM, Correia JR, Cabral-Fonseca S. Durability of glass fibre reinforced polymer pultruded profiles: comparison between QUV accelerated exposure and natural weathering in a Mediterranean climate. Exp Tech 2013. http://dx.doi.org/10.1111/ext.12055.
[24] Surathi P, Karbhari VM. Hygrothermal effects on durability and moisture kinetics of fiber-reinforced polymer composites. SSRP 2006;6:15.
[25] Grammatikos SA, Zafari B, Evernden MC, Mottram JT, Mitchels JM. Moisture uptake characteristics of a pultruded fibre reinforced polymer flat sheet subjected to hot/wet aging. Polym Degrad Stab 2015;121:407–19.
[26] Grammatikos SA, Evernden M, Mitchels J, Zafari B, Mottram JT, Papanicolaou GC. On the response to hygrothermal aging of pultruded FRPs used in the civil engineering sector. Mater Des 2016;96:283–95.
[27] Alawsi G, Aldajah S, Rahmaan SA. Impact of humidity on the durability of E-glass/polymer composites. Mater Des 2009;30(7):2506–12.
[28] Sauvant-Moynot V, Duval S, Grenier J. Innovative pipe coating material and process for high temperature fields. Oil Gas Sci Technol 2002;57(3):269–79.
[29] Jefferson GD, Farah B, Hempowicz ML, Hsiao K-T. Influence of hygrothermal aging on carbon nanofiber enhanced polyester material systems. Compos Part B Eng 2015;78:319–23.
[30] Han SO, Ahn HJ, Cho D. Hygrothermal effect on henequen or silk fiber reinforced poly(butylene succinate) biocomposites. Compos Part B Eng 2010;41(6):491–7.
[31] Del Saz-Orozco B, Alonso MV, Oliet M, Domínguez JC, Rojo E, Rodriguez F. Lignin particle- and wood flour-reinforced phenolic foams: friability, thermal stability and effect of hygrothermal aging on mechanical properties and morphology. Compos Part B Eng 2015;80:154–61.
[32] Chen Y, Davalos JF, Ray I, Kim H-Y. Accelerated aging tests for evaluations of durability performance of FRP reinforcing bars for concrete structures. Compos Struct 2007;78(1):101–11.
[33] Wan YZ, Luo H, He F, Liang H, Huang Y, Li XL. Mechanical, moisture absorption, and biodegradation behaviours of bacterial cellulose fibre-reinforced starch biocomposites. Compos Sci Technol 2009;69(7):1212–7.
[34] Wan YZ, Wang YL, Huang Y, He BM, Han KY. Hygrothermal aging behaviour of VARTMed three-dimensional braided carbon-epoxy composites under external stresses. Compos Part A Appl Sci Manuf 2005;36(8):1102–9.
[35] Guermazi N, Elleuch K, Ayedi HF. The effect of time and aging temperature on structural and mechanical properties of pipeline coating. Mater Des 2009;30(6):2006–10.
[36] Shen C-H, Springer GS. Moisture absorption and desorption of composite materials. J Compos Mater 1976;10(1):2–20.
[37] Mohd Ishak ZA, Ariffin A, Senawi R. Effects of hygrothermal aging and a silane coupling agent on the tensile properties of injection molded short glass fiber reinforced poly(butylene terephthalate) composites. Eur Polym J 2001;37(8):1635–47.
[38] Scida D, Assarar M, Poilâne C, Ayad R. Influence of hygrothermal ageing on the damage mechanisms of flax-fibre reinforced epoxy composite. Compos Part B Eng 2013;48:51–8.
[39] Lai M, Botsis J, Cugnoni J. Studies of hygrothermal degradation of a single fiber composite: an iterative approach with embedded optical sensors and numerical analysis. Compos Part B Eng 2014;60:577–85.
[40] Williams DH, Fleming I, Pretsch E. Spectroscopic methods. Org Chem 1989;1989.
[41] Hammett LP. Physical Organic Chemistry. New York: McGraw-Hill; 1940.
[42] Carey FA, Sundberg RJ. Advanced organic chemistry: Part A: structure and mechanisms. Springer Science & Business Media; 2007.
[43] Bellenger V, Verdu J. Oxidative skeleton breaking in epoxy–amine networks. J Appl Polym Sci 1985;30(1):363–74.
[44] Monney L, Belali R, Vebrel J, Dubois C, Chambaudet A. Photochemical degradation study of an epoxy material by IR-ATR spectroscopy. Polym Degrad Stab 1998;62(2):353–9.
[45] Pei Y m, Wang K, Zhan M s, Xu W, Ding X j. Thermal-oxidative aging of DGEBA/EPN/LMPA epoxy system: chemical structure and thermal–mechanical properties. Polym Degrad Stab 2011;96(7):1179–86.
[46] Liu F, Yin M, Xiong B, Zheng F, Mao W, Chen Z, et al. Evolution of microstructure of epoxy coating during UV degradation progress studied by slow positron annihilation spectroscopy and electrochemical impedance spectroscopy. Electrochim Acta 2014;133:283–93.
[47] Park C-H, Lee S-J, Lee T-H, Kim H-J. Characterization of an acrylic pressure-sensitive adhesive blended with hydrophilic monomer exposed to hygrothermal aging: assigning cloud point resistance as an optically clear adhesive for a touch screen panel. React Funct Polym 2016;100:130–41.
[48] Xian G, Karbhari VM. Segmental relaxation of water-aged ambient cured epoxy. Polym Degrad Stab 2007;92(9):1650–9.
[49] Wosu SN, Hui D, Daniel L. Hygrothermal effects on the dynamic compressive properties of graphite/epoxy composite material. Compos Part B Eng 2012;43(3):841–55.
[50] Yang B, Zhang J, Zhou L, Wang Z, Liang W. Effect of fiber surface modification on the lifetime of glass fiber reinforced polymerized cyclic butylene terephthalate composites in hygrothermal conditions. Mater Des 2015;85:14–23.
[51] Golchin A, Wikner A, Emami N. An investigation into tribological behaviour of multi-walled carbon nanotube/graphene oxide reinforced UHMWPE in water lubricated contacts. Tribol Int 2016;95:156–61.
[52] Meng M, Rizvi MJ, Grove SM, Le HR. Effects of hygrothermal stress on the failure of CFRP composites. Compos Struct 2015;133:1024–35.
[53] Meng M, Rizvi MJ, Le HR, Grove SM. Multi-scale modelling of moisture diffusion coupled with stress distribution in CFRP laminated composites. Compos Struct 2016;138:295–304.
[54] Zhong Y, Joshi SC. Initiation of structural defects in carbon fiber reinforced polymer composites under hygrothermal environments. J Compos Mater 2015;50(8):1085–97.